

# AMCoR

Asahikawa Medical College Repository <http://amcor.asahikawa-med.ac.jp/>

BIOLOGICAL and PHARMACEUTICAL BULLETIN (2006) 29(3):437–442.

Decreases in pheromonal responses at the accessory olfactory bulb of mice with a deficiency of the  $\alpha_1\text{B}$  or  $\beta_3$ -subunits of voltage-dependent  $\text{Ca}^{2+}$ -channels

Murakami M, Matsui H, Shiraiwa T, Suzuki T, Sasano H, Takahashi E, Kashiwayanagi M

Regular article (Revised)

Decreases in pheromonal responses at the accessory olfactory bulb of mice with a deficiency of the  $\alpha_{1B}$  or  $\beta 3$  subunits of voltage-dependent  $\text{Ca}^{2+}$ -channels

<sup>a</sup>Manabu Murakami, <sup>b</sup>Hitosi Matsui, <sup>c</sup>Takeshi Shiraiwa, <sup>d</sup>Takashi Suzuki, <sup>d</sup>Hironobu Sasano, <sup>e</sup>Eiki Takahashi and <sup>b</sup>Makoto Kashiwayanagi

<sup>a</sup>Department of Pharmacology, Akita University School of Medicine, Akita 010-8543, Japan, <sup>b</sup>Department of Sensory Physiology, Asahikawa Medical College, Asahikawa 078-8510, Japan, <sup>c</sup>Graduate School of Pharmaceutical Sciences, Hokkaido University, Sapporo 060-0812, Japan, <sup>d</sup>Department of Pathology, Tohoku University School of Medicine, Sendai 980-8575, Japan, <sup>e</sup>Tsukuba Research Laboratory, Eisai Co., Ltd, Tsukuba 300-2635, Japan

Correspondence to Makoto Kashiwayanagi, Department of Sensory Physiology, Asahikawa Medical College, Asahikawa 078-8510, Japan, e-mail: yanagi@asahikawa-med.ac.jp

柏柳誠、078-8510 旭川市緑が丘東2条1丁目 旭川医科大学生理学第二講座  
電話 0166-68-2330、FAX 0166-68-2339、e-mail: yanagi@asahikawa-med.ac.jp

Pheromones affect gonadal functions and sexual behaviors. Information in regard to pheromones is received by the vomeronasal organ (VNO) and transmitted to the accessory olfactory bulb (AOB). We investigated the physiological role of the  $\alpha_{1B}$  and  $\beta_3$  subunits of the N (neuronal)-type voltage-dependent  $Ca^{2+}$  channel in the neurotransduction in the accessory olfactory (vomeronasal) system using  $\alpha_{1B}$ -deficient mice and  $\beta_3$ -deficient mice. RT-PCR studies showed the existence of  $\beta_1$ ,  $\beta_2$ ,  $\beta_3$ ,  $\beta_4$ ,  $\alpha_{1A}$ ,  $\alpha_{1B}$ , and  $\alpha_{1C}$  subunits of voltage-dependent  $Ca^{2+}$  channels in the mouse VNO. Immunohistochemical studies showed that the  $\alpha_{1A}$ ,  $\alpha_{1B}$ , and  $\alpha_{1C}$  subunits of voltage-dependent  $Ca^{2+}$  channels exist in the sensory neurons and supporting cells of the mouse VNO. Exposure of the VNO to urine samples excreted from male mice induced lower Fos-immunoreactivity in the periglomerular (PG) cells of the AOBs in  $\alpha_{1B}$ -deficient female mice than in those of wild mice. The density of Fos-immunoreactive (Fos-ir) cells after exposure to female urine samples at the periglomerular cell layer of  $\alpha_{1B}$ -deficient male mice was lower than that of wild mice. Exposure of the VNO of  $\beta_3$ -deficient female mice to male urine samples also induced low Fos-ir cells in the periglomerular cell layer of the AOB. These data suggest the importance of the  $\alpha_{1B}$  and  $\beta_3$  subunits of the N-type voltage-dependent  $Ca^{2+}$  channel for the pheromone signal transduction system.

Keywords: N-type  $\text{Ca}^{2+}$  channel,  $\alpha_{1B}$  subunit,  $\beta 3$  subunit, accessory olfactory bulb, pheromonal response

## Introduction

Pheromonal signals provide specific information concerning the identity, gender, and endocrine and social status of different members of the population in a variety of mammals<sup>1-5)</sup>. The vomeronasal system is a chemosensory system organized in parallel with the main olfactory system in most terrestrial vertebrates. The interaction of a pheromone with the receptive membrane of vomeronasal sensory neurons (VSN) initiates a sequential molecular event leading to action potential initiation<sup>6,7)</sup>, which transmits pheromonal information to neurons in the accessory olfactory bulb (AOB) via synapses<sup>7)</sup>.

Classic electrophysiological studies indicate that there are at least six functionally distinct  $\text{Ca}^{2+}$  channel subtypes: L-, N-, P-, Q-, R- and T-type. The N-type and P/Q-type  $\text{Ca}^{2+}$  channels play a predominant role in neurotransmitter release<sup>8)</sup>. Voltage-dependent calcium channels are comprised of five subunits,  $\alpha_1$ ,  $\alpha_2$ ,  $\delta$ ,  $\beta$ , and  $\gamma$ <sup>9,10)</sup>. The  $\text{Cav}2.2$  ( $\alpha_{1B}$ ) subunit is the pore-forming subunit in the neuronal (N)-type channels. The  $\beta$  subunits are located on the intracellular side of the membrane, increase the channel population, and influence the coupling of gating charge movement. The  $\alpha_{1B}$  and  $\beta_3$  subunits, abundantly expressed in the brain, form a major part of the N-type  $\text{Ca}^{2+}$  channel, which are expressed in the presynaptic active zone<sup>11-13)</sup>,

suggesting that both subunits play significant roles in the synaptic transmission.

To explore the physiological roles of the N-type  $\text{Ca}^{2+}$  channel in the transmission of pheromonal information from the VSN to neurons in the AOB, we examined neuronal activities in the AOB using Fos-immunohistochemical methods. Pheromones have been found in saliva, skin gland secretions, and urine. In the periglomerular (PG) cell layer of the AOB,  $\alpha_{1B}$ -deficient mice and  $\beta 3$ -deficient mice showed a decrease in Fos immunoreactions to urine samples, suggesting decreased neural activities in response to urinary pheromones by the ablation of the  $\alpha_{1B}$  and  $\beta 3$  genes. Our data suggests the involvement of the  $\alpha_{1B}$  and  $\beta 3$  subunits and the N-type  $\text{Ca}^{2+}$  channel in the pheromone neurotransduction pathway.

## **Materials and methods**

### *Animals*

All experiments were carried out in accordance with the Guidelines for the Use of Laboratory Animals of the Asahikawa Medical College and Graduate School of Pharmaceutical Sciences, Hokkaido University. The  $\alpha_{1B}$ -deficient mice ( $\alpha^{-/-}$ ) and  $\beta 3$ -deficient mice ( $\beta 3^{-/-}$ ) were constructed from genomic DNA clones, as reported previously<sup>14,15</sup>. The wild-type ( $\alpha^{+/+}$  and  $\beta 3^{+/+}$ ),  $\alpha^{-/-}$  and  $\beta 3^{-/-}$  mice were 12-15 weeks

of age, and were maintained at  $22 \pm 0.5^\circ \text{C}$  and 58% relative humidity with a 12-h light/12-h dark cycle (lights off at 21:00). The males and females were housed in the same room with free access to food and water. Three or four mice were used under each condition, and all animals were used only once. All experiments were conducted during the light phase of the cycle.

#### *RNA Isolation and RT-PCR*

Total RNA was isolated from tissues of the vomeronasal organ (VNO) using an RNeasy extraction kit (Qiagen Inc., Valencia, CA). Reverse transcription reactions were performed in a solution of 10 pmol oligo-dT primer, 1  $\mu\text{g}$  RNA, 1 x first strand cDNA buffer (Life Technologies, Rockville, MD), 10 mM dithiothreitol, 0.4 mM dNTPs, 40 U RNAsin, and 200 U Superscript II (Life Technologies) in a volume of 25  $\mu\text{l}$ , at  $42^\circ\text{C}$  for 45 min. For the RT-PCR reaction, 2.0  $\mu\text{l}$  was used in PCR assays.

The  $\alpha_{1A}$ ,  $\alpha_{1B}$ , and  $\alpha_{1C}$  subunit-specific sequences were amplified by PCR with the primers as described previously <sup>16</sup>): A1A1, 5'-CTC CCG AGA ACA GCC TTA TC-3' and for A1A2, 5'-GTC TGC CTC CTC TTC CTC TTT CTT C-3', which correspond to the sequences of the murine  $\alpha_{1A}$  subunits T<sub>403</sub>PENSLIVT<sub>411</sub> and E<sub>463</sub>KKEEEEEAD<sub>471</sub>; A1B1, 5'-GGG GAT AAG GAA ACC CGA AAT CAC CA-3' and for A1B2, 5'-CTT

GGC CTT CCA GGT TCA TGT TAC CA-3', which correspond to the sequences of the murine  $\alpha_{1B}$  subunit G<sub>319</sub>DKETRNHQ<sub>327</sub> and G<sub>403</sub>NMNLEGQA<sub>411</sub>; A1C3, 5'-TTG GCC ATT GCG GTG GAC AAC CTG -3' and for A1C4, 5'-CTG GAG TGC ATC CAT GTG TAT CTT G -3', which correspond to the sequences of the murine  $\alpha_{1C}$  subunit L<sub>510</sub>AIAVDNL<sub>517</sub> and T<sub>580</sub>KIHMDALQ<sub>588</sub>.

The  $\beta_1$ ,  $\beta_2$ ,  $\beta_3$  and  $\beta_4$  subunit-specific sequences were amplified by PCR with the specific primers: MB1S, 5'-GTC AAA CTG GAC AGC CTT CGT -3', and MB1A, 5'-GAC ACT GCT CAC GCT AGT CTT -3', which correspond to the sequences of the murine  $\beta_1$  subunits V<sub>163</sub>RKLD<sub>SLR</sub><sub>169</sub> and K<sub>240</sub>TSVSSVP<sub>246</sub>; MB2S, 5'-CTA GAG AAC ATG AGG CTA CAG -3', and MB2A, 5'-ACT GTT TGC ACT GGG CTT AGG -3', which correspond to the sequences of the murine  $\beta_2$  subunit L<sub>131</sub>ENMRLQ<sub>137</sub> and P<sub>198</sub>KPSANS<sub>204</sub>; MB3S, 5'-CTC AAA CAG GAA CAG AAG GCC -3', and MB3A, 5'-CAT AGC CTT TCA GAG AGG GTC -3', which correspond to the sequences of the murine  $\beta_3$  subunits L<sub>129</sub>KQEQKAR<sub>135</sub> and P<sub>186</sub>SLKGYE<sub>192</sub>; MB4S, 5'-CTG AGC CTT TCA GAG AGG GTC -3', and MB4A, 5'-CAT TGA CGG CAC GAC GTC ATA -3', which correspond to the sequences of the murine  $\beta_4$  subunits L<sub>154</sub>RLENIR<sub>160</sub> and Y<sub>213</sub>DVVPSM<sub>219</sub>.



### *Immunohistological distribution of the voltage-dependent calcium channels*

Immunohistological analysis was performed using the streptavidin-biotin amplification method as described previously <sup>16)</sup>. The dilutions of primary antibodies used in our study were as follows: 1/100, 1/100 and 1/400, for  $\alpha_{1A}$ ,  $\alpha_{1B}$  and  $\alpha_{1C}$ , respectively. Normal goat serum (1%) was applied to the sections for 20 min at room temperature, and then the primary antibody was reacted to the sections for 18 h at 4 °C. Commercially available antibodies that specifically recognize  $\alpha_{1A}$ ,  $\alpha_{1B}$  and  $\alpha_{1C}$  subunits (Alomone, Jerusalem, Israel) were used. Sections were reacted with Envision plus (DAKO, Copenhagen, Denmark). The antigen-antibody complex was visualized as brown precipitation with 3.3'-diaminobenzidine (DAB) solution (1 mM DAB, 50 mM Tris-HCl buffer (pH 7.6), and 0.006% H<sub>2</sub>O<sub>2</sub>) and counterstained with hematoxylin.

### *Fos- Immunohistochemistry*

Immunohistochemical experiments were carried out as described previously <sup>7)</sup>. The animals, all of whom were deeply anesthetized with pentobarbital sodium (150 mg/kg), were perfused through the heart with phosphate-buffered saline (PBS), followed by fixation with 4% paraformaldehyde. The olfactory bulbs along with the brain were removed and soaked in the same fixative solution overnight, and then cut

serially on a vibratome at a thickness of 50  $\mu\text{m}$ . The free-floating sagittal sections were first treated with 0.3%  $\text{H}_2\text{O}_2$  for 15 min in PBS with 0.4% Triton X-100 (PBSx), followed by two washes of PBSx. After a 1-h incubation in 3% normal goat serum, the sections were incubated with c-Fos polyclonal antibody (1:8000, Ab-5; Oncogene Research Products, Cambridge, MA) in PBSx for 24 h at room temperature. The sections were then rinsed in PBSx and incubated with biotinylated goat anti-rabbit IgG (1:200; Vector, Burlingame, CA) for 1 h, respectively. The sections were rinsed again in PBSx, incubated with ABC (ABC Elite Kit; Vector) for 1 h, and developed with DAB/ $\text{H}_2\text{O}_2$  (0.05% DAB and 0.003%  $\text{H}_2\text{O}_2$  in 0.05 M Tris-HCl buffer) for 12 min. The sections were then rinsed with water and mounted. Different pheromonal information of sex and strains received by two populations of sensory neurons in the VNO was projected to the rostral and caudal regions of the glomerular layer of the AOB in rodents <sup>6,7</sup>. All Fos-ir cells at the caudal and rostral regions in the AOB were counted under a microscope. To estimate the density of the Fos-ir cells, the area of the PG layer, the mitral/tufted cell layer and the granule cell layer in photographs were measured. The sections were analyzed in a blind fashion.

#### *Stimulation with urine preparations*

The noses of mice were subjected to a spray of urine preparations from male or

female mice, or to a salt solution (control). The mice were gently held in place manually during the spraying of urinary samples (30 ml) without anesthetic for 30 min, and then sacrificed. Urine was collected from 4-10 mice using a metabolic cage. The control salt solution, which has an ionic composition similar to urine, consisted of (in mM): 150 NaCl, 300 KCl, 1 CaCl<sub>2</sub>, 3 MgCl<sub>2</sub>, and 10 HEPES-NaOH, pH 7.6. Urine was diluted to 1/10 or 1/2 with the control salt solution.

#### *Statistical analyses*

Three-way ANOVA was used to test differences between the two groups of mice (wild and knockout), categories of stimulation (control salt solution and urine preparation) and regions of the AOB (caudal and rostral halves). Post-hoc analyses (Fisher's PLSD) were used to evaluate differences between values for each factor. Analyses were carried out using StatView software (SAS Institute Inc., Cary, NC).

## **Results**

#### *RT-PCR analysis in the mouse VNO*

We analyzed the RNA transcripts of the  $\alpha_1$  and  $\beta$  subunits by RT-PCR to investigate the expression of the subunits of the voltage-dependent Ca<sup>2+</sup> channel in the

VNO. Fragments of 252, 222, 187, 195, 204, 273, and 237 bp were generated, which corresponded to the  $\beta_1$ ,  $\beta_2$ ,  $\beta_3$ ,  $\beta_4$ ,  $\alpha_{1A}$ ,  $\alpha_{1B}$  and  $\alpha_{1C}$  subunit-specific fragments, respectively (Fig. 1). As the  $\alpha_{1A}$ ,  $\alpha_{1B}$  and  $\alpha_{1C}$  subunits compose P/Q-, N- and L-type  $\text{Ca}^{2+}$  channels, respectively<sup>9)</sup>, the results of the RT-PCR analysis suggested the presence of various types of  $\text{Ca}^{2+}$  channels in the VNO and the involvement of the voltage-dependent  $\text{Ca}^{2+}$  channels in the pheromonal signal transduction system. As  $\beta$  subunits are known to modify  $\text{Ca}^{2+}$  currents, they might regulate pheromonal signal transduction. There was null amplification of  $\beta_3$  subunit in the  $\beta_3^{-/-}$ , while no difference in the PCR amplifiable products of other subunits were detected. We also analyzed other  $\alpha_{1D}$ ,  $\alpha_{1E}$ ,  $\alpha_{1F}$  and  $\alpha_{1G}$  subunits, but no PCR products were amplified, suggesting that these subunits made at most a minor contribution.

#### *Immunohistological analysis of various voltage-dependent calcium channel $\alpha_1$ subunits*

To investigate the distribution of P/Q-, N-, L-, and R-type calcium channels in the VNO, we examined immunostaining using anti- $\alpha_{1A}$  ( $\text{Ca}_V2.1$ ), - $\alpha_{1B}$  ( $\text{Ca}_V2.2$ ) and - $\alpha_{1C}$  ( $\text{Ca}_V1.2$ ) subunit antibodies with immunohistochemistry (Fig. 2). There was moderate immunostaining of the P/Q-type channel-forming subunit  $\alpha_{1A}$  in the VNO (Fig. 2A). Immunostaining was observed throughout the vomeronasal sensory

epithelium. Immunostaining at the luminal site of the supporting cells (arrows) showed intense expression, while moderate expression was also detected in the sensory neurons (asterisks). A significant decrease in staining of  $\alpha_{1A}$  was detected in the  $\beta 3$ -deficient mice (Fig. 2B). The N-type forming  $\alpha_{1B}$  subunit showed a distribution pattern similar to that of the  $\alpha_{1A}$  subunit (Fig. 2C). The immunostaining of the luminal side was immunopositive (arrows), and moderate expression in the sensory neurons was also observed (asterisks). The expression level of the  $\alpha_{1B}$  subunit in the  $\beta 3$ -deficient mice was significantly decreased in both areas (Fig. 2D). Immunostaining for the L-type channel-forming  $\alpha_{1C}$  was observed mainly in the sensory neurons (arrows in Fig. 2E). There were no significant differences between wild and mutant mice (Fig. 2F).

#### *Fos-immunoreactive cells in the AOB*

Induction of c-Fos has been widely used as an assay for studying the excitability of populations of neurons within many different brain regions, including the AOB<sup>7,17</sup>. To analyze the effect of the ablation of the  $\alpha_{1B}$  subunit on the transmission of pheromonal information, we determined the number of Fos-immunoreactive (Fos-ir) cells in the AOB, where primary afferent fibers from the VSNs innervate. Exposure to

diluted urine (1:10) from male mice induced a marked increase in the production of Fos-ir cells in the AOB of the  $\alpha_{1B}^{+/+}$  female mice (Fig. 3B). Fos-ir cells were found in the mitral/tufted cell layer, granule cell layer, and periglomerular cell layer (PGL). The greatest density of labeled cells was observed in the granule cell layer. The number of Fos-immunoreactive cells in  $\beta 3^{+/+}$  mice after exposure to male urine was larger than after exposure to the control salt solution. This result indicates that urine was able to induce a remarkable level of expression of Fos-immunoreactive cells under our experimental conditions.

The density of Fos-ir cells at the rostral and caudal regions of  $\alpha_{1B}^{+/+}$  and  $\alpha_{1B}^{-/-}$  female mice was analyzed with three-way ANOVA. In the mitral/tufted cell layer and granule cell layer, there were no significant differences between mice exposed to the control salt solution and those exposed to urine samples, or between  $\alpha_{1B}^{+/+}$  and  $\alpha_{1B}^{-/-}$  female mice (data not shown). Therefore, we focused on the Fos-ir cells at the PGL in further analyses. Figure 4 shows the density of Fos-ir cells (number/ $\mu\text{m}^2$ ) at the PGL after exposure to the control salt solution and male urine samples. Three-way ANOVA was used to compare the densities of Fos-ir cells between mice exposed to the control salt solution and those exposed to urine samples ( $F(1, 24) = 11.71, P = 0.0022$ ), between  $\alpha_{1B}^{+/+}$  and  $\alpha_{1B}^{-/-}$  female mice ( $F(1, 24) = 20.724, P = 0.0001$ ), and between the rostral

and caudal regions ( $F(1, 24) = 1.562, P = 0.2235$ ). There was an interaction between the stimulating condition and mice ( $P = 0.0095$ ). A post-hoc test indicated that there were significant differences in the densities of Fos-ir cells between exposure to the control salt solution and exposure to urine preparation at both the rostral ( $P = 0.0049$ ) and the caudal ( $P = 0.00172$ ) regions of  $\alpha_{1B}^{+/+}$  female mice. However, there were no such significant differences in  $\alpha_{1B}^{-/-}$  female mice.

Just as female mice respond to male pheromones, male mice also respond to female pheromones. Therefore, we also examined Fos-ir cells at the PGL of the AOB of  $\alpha_{1B}^{+/+}$  and  $\alpha_{1B}^{-/-}$  male mice after exposure to urine excreted from female mice (Fig. 5). Three-way ANOVA was used to compare the densities of Fos-ir cells between mice exposed to the control salt solution and those exposed to urine samples ( $F(1, 16) = 14.235, P = 0.0017$ ), between  $\alpha_{1B}^{+/+}$  and  $\alpha_{1B}^{-/-}$  male mice ( $F(1, 24) = 2.371, P = 0.1431$ ), and between the rostral and caudal regions ( $F(1, 24) = 0.029, P = 0.8675$ ). In the rostral region of  $\alpha_{1B}^{+/+}$  male mice, the density of Fos-ir cells after exposure to a urine preparation was about 5 times larger than that after exposure to the control salt solution ( $P = 0.0391$ ). In  $\alpha_{1B}^{-/-}$  males, however, there was no significant difference in the density of Fos-ir cells between those exposed to the control salt solution and those exposed to the urine preparation.

N-type  $\text{Ca}^{2+}$  channels are made up primarily of  $\alpha_{1B}$  and  $\beta 3$  subunits. We explored the roles of  $\beta 3$  subunits in the pheromonal transduction in the vomeronasal system using  $\beta 3$  subunit-deficient mice ( $\beta 3^{-/-}$ ). The exposure of female mice to urine diluted 1:10 did not significantly increase the number of Fos-ir cells at the PGL, mitral/tufted cell layer, or granule cell layer of  $\beta 3^{+/+}$  or  $\beta 3^{-/-}$  female mice (data not shown). Therefore, we stimulated the VNO of female mice with urine diluted 1:2. Figure 6 shows the density of Fos-ir cells (number/ $\mu\text{m}^2$ ) at the PGL of the AOB of  $\beta 3^{+/+}$  and  $\beta 3^{-/-}$  female mice after exposure to the control salt solution and male urine samples. Three-way ANOVA was used to compare the densities of Fos-ir cells between mice exposed to the control salt solution and those exposed to urine samples ( $F(1, 18) = 33.673, P < 0.0001$ ), between  $\beta 3^{+/+}$  and  $\beta 3^{-/-}$  female mice ( $F(1, 18) = 0.514, P = 0.4826$ ), and between the rostral and caudal regions ( $F(1, 18) = 36.577, P < 0.0001$ ). There was an interaction between the type of exposure and the region ( $P = 0.0001$ ). A post-hoc test indicated that there were significant differences in the densities of Fos-ir cells between mice exposed to the control salt solution and those exposed to the urine preparation in both  $\beta 3^{+/+}$  ( $P < 0.0001$ ) and  $\beta 3^{-/-}$  ( $P = 0.001$ ) female mice at the rostral region.

## Discussion



In the present study, we confirmed the presence of the  $\beta 1$ ,  $\beta 2$ ,  $\beta 3$ ,  $\beta 4$ ,  $\alpha_{1A}$ ,  $\alpha_{1B}$  and  $\alpha_{1C}$  subunits of voltage-dependent  $\text{Ca}^{2+}$  channels in the vomeronasal sensory epithelium, and investigated the roles of  $\alpha_{1B}$  and  $\beta 3$  of N-type  $\text{Ca}^{2+}$  channel in the transmission of pheromonal information to the AOB using mice without  $\alpha_{1B}$  or  $\beta 3$  subunits. We showed that neural activities, which were monitored with Fos-immunoreactivities, after exposure to urine samples in the mice without  $\alpha_{1B}$  or  $\beta 3$  subunits were lowered compared to those in wild mice.

#### *Roles of N-type $\text{Ca}^{2+}$ channel in the transduction of pheromonal information*

The VNSs give rise to afferent sensory fibers of the vomeronasal nerve and innervate into the AOB<sup>18)</sup>. The terminals of the vomeronasal nerve fibers make excitatory synaptic contacts with dendrites of the mitral/tufted output cells within the glomeruli of the AOB<sup>19)</sup>. The activity of mitral cells is modulated by several types of interneurons, chief among them the granule and PG cells<sup>20)</sup>. The mitral cells form reciprocal dendrodendritic synapses with granule cells, the main class of interneuron in the AOB<sup>21)</sup>. Granule cell synapses are depolarized by an excitatory amino acid input from the mitral cells, and in turn provide a feedback inhibition to the mitral cells via GABA release<sup>21)</sup>. In the present study, ablation of the  $\alpha_{1B}$  and  $\beta 3$  subunits of the

voltage-dependent calcium channel did not induce decreases in the number of Fos-ir cells after exposure to urinary pheromones at the mitral/tufted cell layer or granule cell layer (data not shown). In the cerebellum, P/Q-type  $\text{Ca}^{2+}$  channel  $\alpha_{1A}$  subunit gene expression is upregulated in N-type  $\alpha_{1B}$ -deficient mice<sup>15)</sup>. It is, therefore, possibly a consequence of compensation by another  $\text{Ca}^{2+}$  channel  $\alpha_1$  subunit(s) in neurons in the vomeronasal system.

The PG cells of the AOB receive input from the VSN and form dendrodendritic synapses with each other and with mitral cells<sup>20)</sup>. In the AOB, PG cells are mainly GABAergic<sup>22)</sup> and are considered to be inhibitory interneurons. As shown in the present study, ablation of the  $\alpha_{1B}$  or  $\beta_3$  subunits decreased the neural activities induced by urinary pheromones at the periglomerular cell layer (Figs. 3, 4, 5 and 6). In the neural circuit of the AOB, the N-type  $\text{Ca}^{2+}$  channels, which are made up of primarily  $\alpha_{1B}$  and  $\beta_3$  subunits, play a significant role in the release of neurotransmitters during the transmission and treatment of pheromonal information.

As shown in the present study, both the  $\alpha_{1A}$  (P/Q-type channel) and  $\alpha_{1B}$  (N-type channel) subunits were decreased in the VNO of the  $\beta_3$ -deficient mice (Fig. 2). In a previous study using  $\beta_3$ -deficient mice, we found that the number of N-type channel was decreased to ca. 50% in the dorsal root ganglion neurons<sup>16)</sup>. Given that the

number of N-type channel in the VNO is decreased to 50 %, like in dorsal root ganglion, the similar phenotype of the  $\beta 3$ -deficient mouse in the Fos-ir analysis just like N-type deficient mouse might not be due to the mere 50 % reduction of N-type channel. In this sense, the decreased amount of  $\alpha 1A$  subunit in the immunostaining may have been related to the decreased number of Fos-ir cells in the  $\beta 3$ -deficient mice, as P/Q-type channel are also located at the presynapses <sup>8)</sup>.

As shown in previous studies, pheromonal information received at Gi-expressing sensory neurons at the apical layer and Go-expressing sensory neurons at the basal layer in the vomeronasal sensory epithelium are transmitted to the rostral and caudal regions of the AOB, respectively <sup>6,7,23)</sup>. These subregions receive different pheromonal information from VSN <sup>7,24-26)</sup>. In the present study, however, there were no significant differences in the degree of decreases in neural activities in response to urinary pheromones of  $\alpha_{1B}$ -deficient mice or  $\beta 3$ -deficient mice at the caudal and rostral regions of the AOB. These results suggest that there is no remarkable difference in the contribution of N-type  $Ca^{2+}$  channel to the synaptic transmission at the caudal and rostral regions in the AOB.

*Subunits of N-type  $Ca^{2+}$  channel in the VNO*

In the present study, we showed that the  $\alpha_{1B}$  subunit was expressed in the vomeronasal systems (Figs. 1 and 2). In the vomeronasal sensory epithelium, not only sensory neurons but also supporting cells, i.e., glial cells, have  $\alpha_{1B}$  subunits. It has been reported that glial cells, such as astrocytes<sup>27)</sup> and muller cells<sup>28)</sup>, express multiple types of voltage-gated  $\text{Ca}^{2+}$  channels, including N-type  $\text{Ca}^{2+}$  channel. Therefore, it is possible that N-type  $\text{Ca}^{2+}$  channel, which are expressed in the supporting cells of the vomeronasal sensory epithelium, function in the regulation of pheromonal reception.

Using a voltage clamp, Inamura et al. identified a voltage-dependent  $\text{Na}^+$  inward current, an inward  $\text{Ca}^{2+}$  current, a sustained outward  $\text{K}^+$  current, and a  $\text{Ca}^{2+}$ -activated  $\text{K}^+$ -current in rat VSN<sup>29)</sup>. In the frog VSN, a voltage-dependent  $\text{Ca}^{2+}$  current was observed in iso-osmotic  $\text{BaCl}_2$ <sup>30)</sup>. Although it has not been well characterized, the  $\text{Ca}^{2+}$  current in frog VNO neurons also appears to contain a component of T-type current<sup>30)</sup>.  $\text{Ca}^{2+}$  currents, however, were much more easily recorded in the rat VSN; depolarizing voltage pulses induced a voltage-dependent  $\text{Ca}^{2+}$  current in 10 mM  $\text{CaCl}_2$  external solution and even in normal Tyrode solution containing 2 mM  $\text{CaCl}_2$ <sup>29)</sup>. Liman and Corey showed that the two components of  $\text{Ca}^{2+}$  current in VNO neurons of mice have properties similar to those of T-type and L-type  $\text{Ca}^{2+}$  channels<sup>31)</sup>. L-type and T-type  $\text{Ca}^{2+}$  channels, however, are not normally involved in excitatory transmitter

release<sup>8)</sup>. However, there have been no electrophysiological studies indicating the existence of N-type and/or P/Q type  $\text{Ca}^{2+}$  channels that play a role as key molecules in the neurotransmitter release between VSN and mitral/tufted cells in the AOB. In the present study, we showed the existence of mRNA encoding  $\alpha_{1B}$  and  $\beta 3$  subunits, which probably constitute N-type  $\text{Ca}^{2+}$  channels in the VSN. There were no differences in the Fos-immunoreactivities after exposure to urinary pheromones in the mitral/tufted cells, which directly receive the pheromonal information from the VSN. As described above, it is possible that other  $\alpha_1$  subunit(s) compensate for deficient ( $\alpha_{1B}$ -null mice) and decreased ( $\beta 3$  subunit-null mice) N-type calcium channel.

## **Acknowledgements**

We gratefully thank Profs. Kiyoshi Toko, Veit Flockerzi and Bernd Lindemann for their support and Ikuko Kashiwayanagi for her assistance. This work was supported by a Grant-in-Aid for Scientific Research from the Ministry of Education, Science, and Culture, Japan.

## References

- 1) Powers,J.B., Winans,S.S., *Science*, **187**, 961-963 (1975).
- 2). Halpern,M., *Annu. Rev. Neurosci.*, **10**, 325-362 (1987).
3. Wysocki,C.J., Meredith,M., “Neurobiology of Taste and Smell”, ed. by T.E.Finger and W.L.Silver, New York, 1987.
- 4) Halpern,M., Martinez-Marcos,A., *Prog. Neurobiol.*, **70**, 245-318 (2003).
- 5) Keverne,E.B., *Physiol Behav.*, **83**, 177-187 (2004).
- 6) Inamura,K., Matsumoto,Y., Kashiwayanagi,M., Kurihara,K., *J. Physiol. (Lond. )*, **517**, 731-739 (1999).
- 7). Inamura,K., Kashiwayanagi,M., Kurihara,K., *Eur. J. Neurosci.*, **11**, 2254-2260 (1999).
- 8) Reid,C.A., Bekkers,J.M., Clements,J.D., *Trends Neurosci.*, **26**, 683-687 (2003).
- 9) Hofmann,F., Biel,M., Flockerzi,V., *Annu. Rev. Neurosci.*, **17**, 399-418 (1994).
- 10). Catterall,W.A., *Annu. Rev. Cell Dev. Biol.*, **16**, 521-555 (2000).
- 11) Sher,E., Clementi,F., "Omega-conotoxin-sensitive voltage-operated calcium channels in vertebrate cells," *Neuroscience*, **42**, 301-307 (1991).
- 12) Torri,T.F., Passafaro,M., Clementi,F., Sher,E., *Brain Res.*, **547**, 331-334 (1991).
- 13) Witcher,D.R., De Waard,M., Sakamoto,J., Franzini-Armstrong,C., Pragnell,M., Kahl,S.D., Campbell,K.P., *Science*, **261**, 486-489 (1993).
- 14) Murakami,M., Wissenbach,U., Flockerzi,V., *Eur. J. Biochem.*, **236**, 138-143 (1996).
- 15) Takahashi,E., Ino,M., Miyamoto,N., Nagasu,T., *Mol. Brain Res.*, **124**, 79-87 (2004).

- 16) Murakami,M., Suzuki,T., Nakagawasai,O., Murakami,H., Murakami,S., Esashi,A., Taniguchi,R., Yanagisawa,T., Tan-No,K., Miyoshi,I., Sasano,H., Tadano,T., *Brain Res.*, **903**, 231-236 (2001).
- 17) Guo,J., Zhou,A., Moss,R.L., *Neuroreport*, **8**, 1679-1683 (1997).
- 18) Meisami,E., Bhatnagar,K.P., *Micors. Res. Tec.*, **43**, 476-499 (1998).
- 19) Takami,S., Graziadei,P.P., *J. Comp. Neurol.*, **311**, 65-83 (1991).
- 20) Goldmakher,G.V., Moss,R.L., *Brain Res.*, **871**, 7-15 (2000).
- 21) Brennan,P., Kaba,H., Keverne,E.B., *Science*, **250**, 1223-1226 (1990).
- 22) Takami,S., Fernandez,G.D., Graziadei,P.P.C., *Brain Res.*, **588**, 317-323 (1992).
- 23) Jia,C.P., Halpern,M., *Brain Res.*, **719**, 117-128 (1996).
- 24) Brennan,P.A., Schellinck,H.M., Keverne,E.B., *Neuroscience*, **90**, 1463-1470 (1999).
- 25) Matsuoka,M., Yokosuka,M., Mori,Y., Ichikawa,M., *Neurosci. Res.*, **35**, 189-195 (1999).
- 26) Tsujikawa,K., Kashiwayanagi,M., *Biochem. Biophys. Res. Commun.*, **260**, 222-224 (1999).
- 27) Latour,I., Hamid,J., Beedle,A.M., Zamponi,G.W., Macvicar,B.A., *Glia*, **41**, 347-353 (2003).
- 28) Welch,N.C., Wood,S., Jollimore,C., Stevens,K., Kelly,M.E., Barnes,S., *Glia*, **49**, 259-274 (2005).
- 29) Inamura,K., Kashiwayanagi,M., Kurihara,K., *Chem. Senses*, **22**, 93-103 (1997).
- 30) Trotier,D., Doving,K.B., Rosin,J.F., *Eur. J. Neurosci.*, **5**, 995-1002 (1993).
- 31) Liman,E.R., Corey,D.P., *J. Neurosci.*, **16**, 4625-4637 (1996).



## Figure legends

Figure 1 Expression of the  $\alpha_{1A}$ ,  $\alpha_{1B}$ ,  $\alpha_{1C}$ ,  $\beta_1$ ,  $\beta_2$ ,  $\beta_3$ , and  $\beta_4$  subunits of the voltage-dependent  $\text{Ca}^{2+}$  channels in the mouse VNO. The presence of 204, 273, 237, 252, 222, 187, and 195 bp fragments, which corresponded to the  $\alpha_{1A}$ ,  $\alpha_{1B}$ ,  $\alpha_{1C}$ ,  $\beta_1$ ,  $\beta_2$ ,  $\beta_3$ , and  $\beta_4$  subunit specific fragments, respectively, was confirmed by molecular biological analysis.

Figure 2 Immunohistological distribution of the  $\alpha_{1A}$ ,  $\alpha_{1B}$ , and  $\alpha_{1C}$ , subunits of calcium channels in the VNO of  $\beta_3^{+/+}$  (A, C, E) and  $\beta_3^{-/-}$  (B, D, F) female mice. The antigen-antibody complex was visualized as a brown precipitate, and the tissue sections were counterstained with hematoxylin. Scale bars: 200  $\mu\text{m}$ .

Figure 3 Sagittal sections of the AOB of female mice stained with antibodies to Fos protein after exposure to the control salt solution (A) and diluted urine samples (B) in  $\alpha_{1B}^{+/+}$ , and to the control salt solution (C) and diluted urine samples (D) in  $\alpha_{1B}^{-/-}$ . The rostral portion is on the right. Scale bars: 200  $\mu\text{m}$ .

Figure 4 The density of Fos-ir cells (number/mm<sup>2</sup>) at the rostral and caudal regions in the PGL of the AOB of  $\alpha_{1B}^{+/+}$  and  $\alpha_{1B}^{-/-}$  female mice after exposure to the control salt solution and urine samples. Vertical bars represent the mean  $\pm$  SEM.

Figure 5 The density of Fos-ir cells (number/mm<sup>2</sup>) at the rostral and caudal regions in the PGL of the AOB of  $\alpha_{1B}^{+/+}$  and  $\alpha_{1B}^{-/-}$  male mice after exposure to the control salt solution and urine samples. Vertical bars represent the mean  $\pm$  SEM.

Figure 6 The density of Fos-ir cells (number/mm<sup>2</sup>) at the rostral and caudal regions in the PGL of the AOB of  $\beta 3^{+/+}$  and  $\beta 3^{-/-}$  female mice after exposure to the control salt solution and urine samples. Vertical bars represent the mean  $\pm$  SEM.

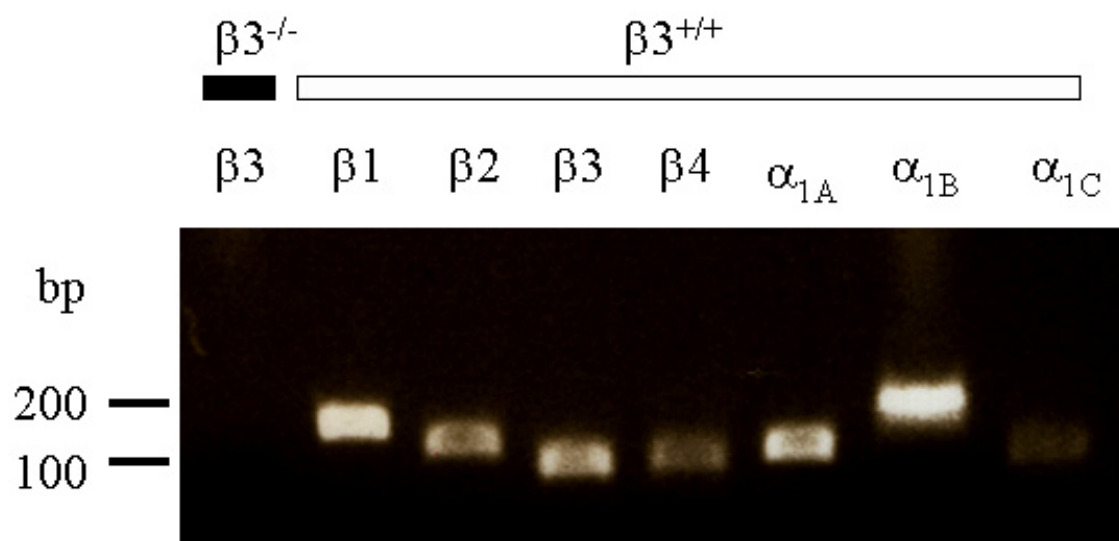


Figure 1 Expression of the  $\alpha_{1A}$ ,  $\alpha_{1B}$ ,  $\alpha_{1C}$ ,  $\beta 1$ ,  $\beta 2$ ,  $\beta 3$ , and  $\beta 4$  subunits of the voltage-dependent  $\text{Ca}^{2+}$  channels in the mouse VNO. The presence of 204, 273, 237, 252, 222, 187, and 195 bp fragments, which corresponded to the  $\alpha_{1A}$ ,  $\alpha_{1B}$ ,  $\alpha_{1C}$ ,  $\beta 1$ ,  $\beta 2$ ,  $\beta 3$ , and  $\beta 4$  subunit specific fragments, respectively, was confirmed by molecular biological analysis.

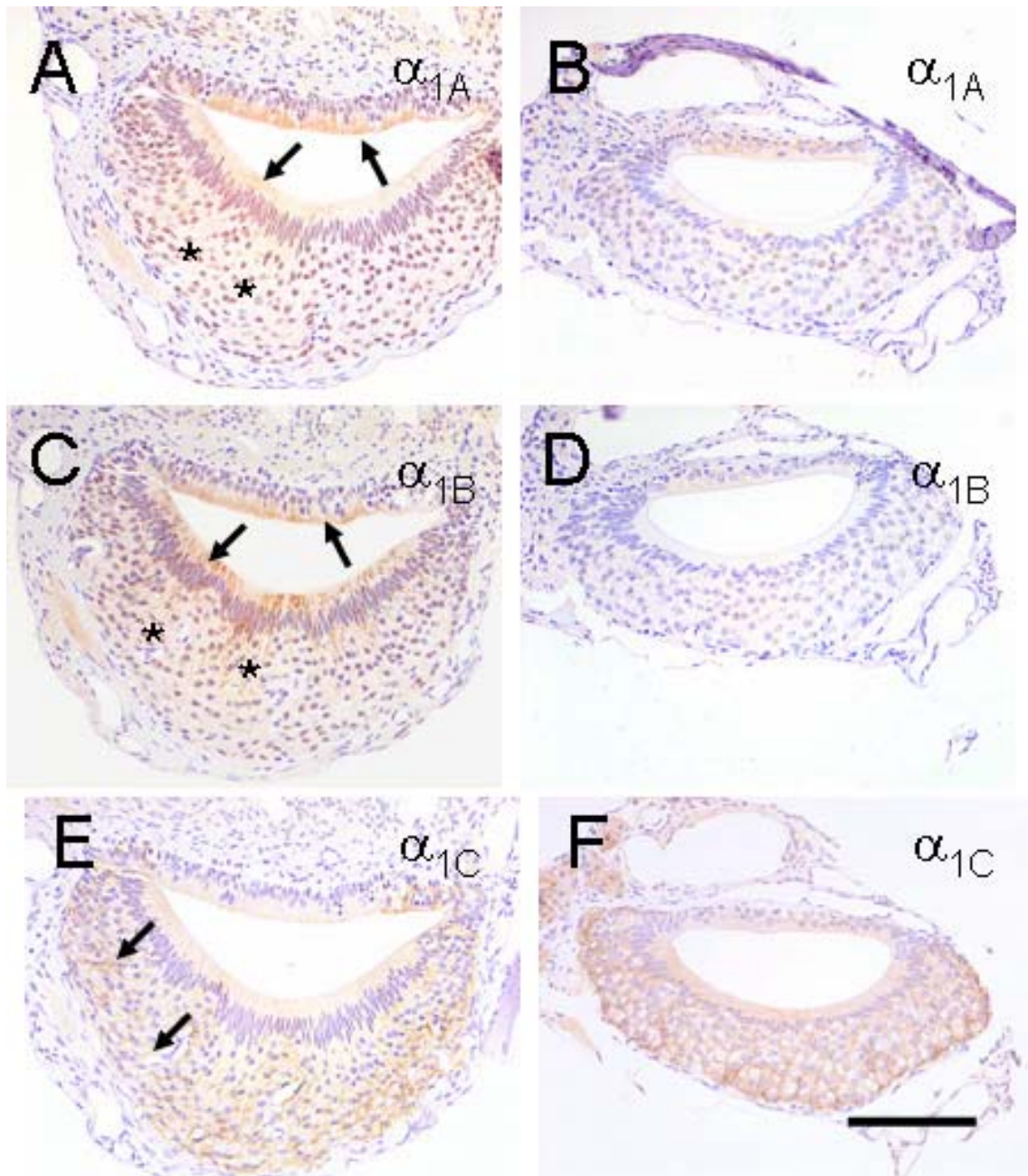


Figure 2 Immunohistological distribution of the  $\alpha_{1A}$ ,  $\alpha_{1B}$ , and  $\alpha_{1C}$ , subunits of calcium channels in the VNO of  $\beta 3^{+/+}$  (A, C, E) and  $\beta 3^{-/-}$  (B, D, F) female mice. The antigen-antibody complex was visualized as a brown precipitate, and the tissue sections were counterstained with hematoxylin. Scale bars: 200  $\mu\text{m}$ .

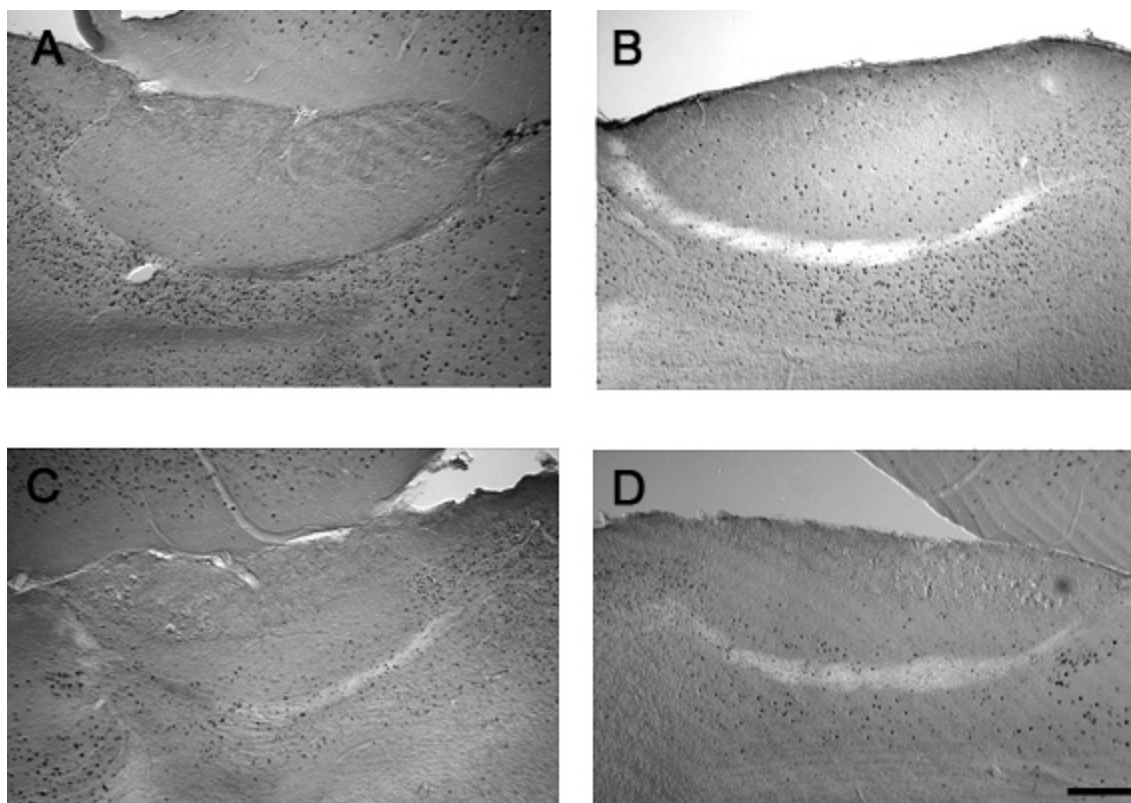


Figure 3 Sagittal sections of the AOB of female mice stained with antibodies to Fos protein after exposure to the control salt solution (A) and diluted urine samples (B) in  $\alpha_{1B}^{+/+}$ , and to the control salt solution (C) and diluted urine samples (D) in  $\alpha_{1B}^{-/-}$ . The rostral portion is on the right. Scale bars: 200  $\mu\text{m}$ .

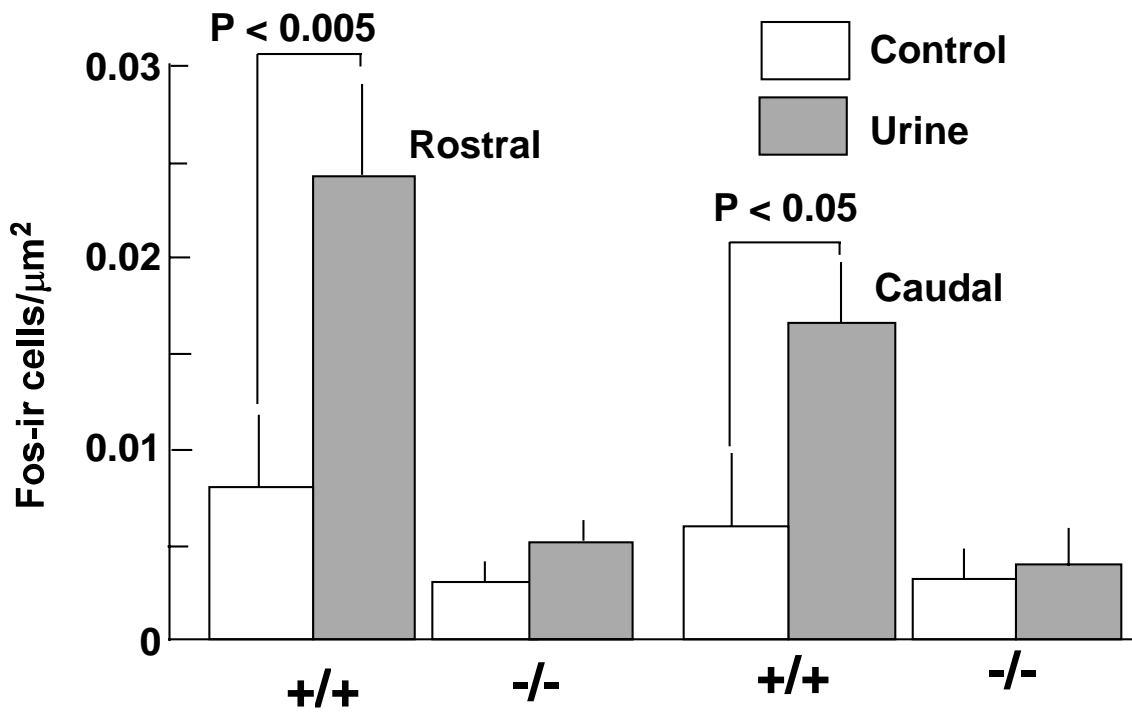


Figure 4 The density of Fos-ir cells (number/ $\text{mm}^2$ ) at the rostral and caudal regions in the PGL of the AOB of  $\alpha_{1B}^{+/+}$  and  $\alpha_{1B}^{-/-}$  female mice after exposure to the control salt solution and urine samples. Vertical bars represent the mean  $\pm$  SEM.

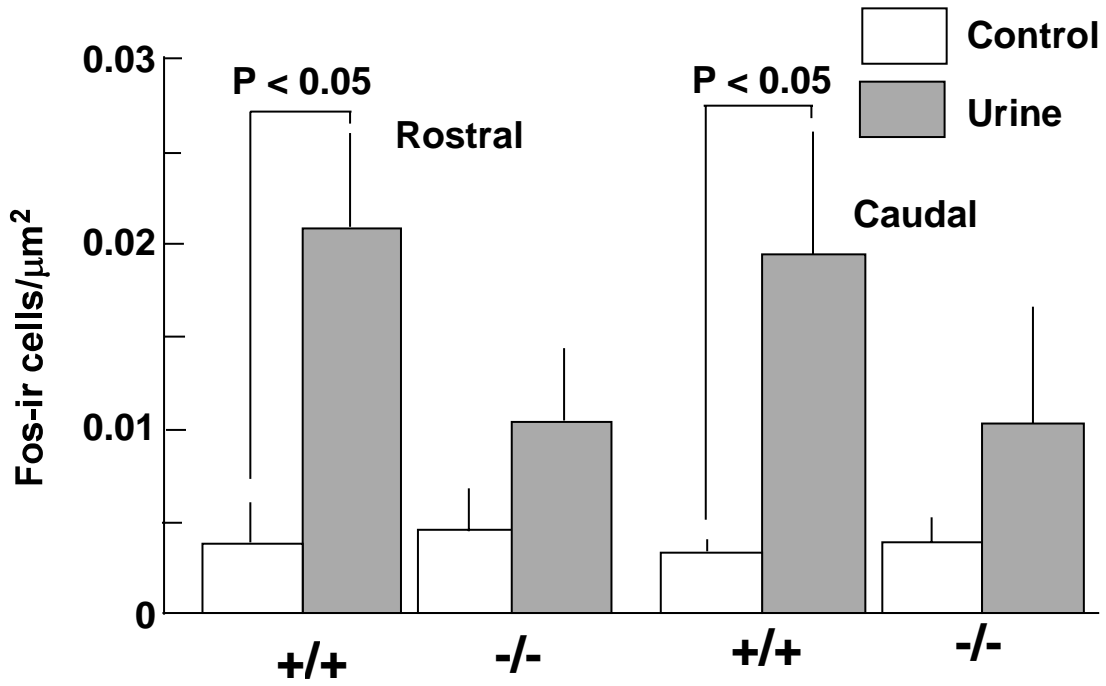


Figure 5 The density of Fos-ir cells (number/ $\text{mm}^2$ ) at the rostral and caudal regions in the PGL of the AOB of  $\alpha_{1B}^{+/+}$  and  $\alpha_{1B}^{-/-}$  male mice after exposure to the control salt solution and urine samples. Vertical bars represent the mean  $\pm$  SEM.

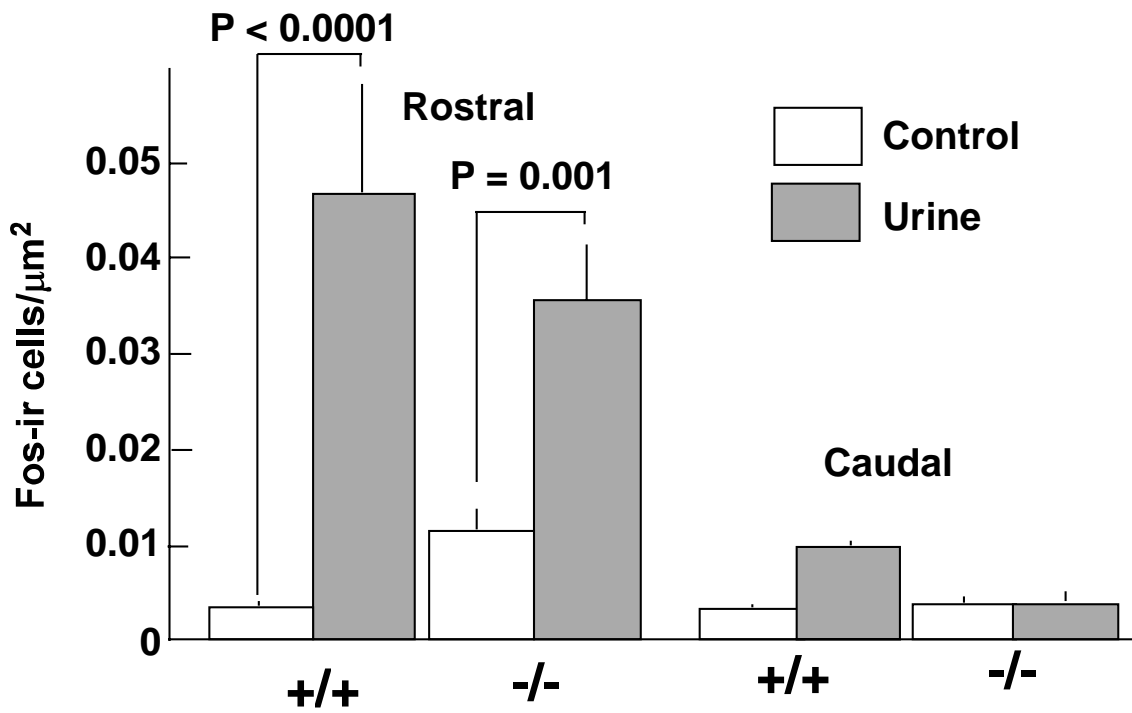


Figure 6 The density of Fos-ir cells (number/mm<sup>2</sup>) at the rostral and caudal regions in the PGL of the AOB of  $\beta 3^{+/+}$  and  $\beta 3^{-/-}$  female mice after exposure to the control salt solution and urine samples. Vertical bars represent the mean  $\pm$  SEM.



$\beta 3^{-/-}$  $\beta 3^{+/+}$  $\beta 3$  $\beta 1$  $\beta 2$  $\beta 3$  $\beta 4$  $\alpha_{1A}$  $\alpha_{1B}$  $\alpha_{1C}$ 

bp

200

100

